Pol. J. Environ. Stud. Vol. 22, No. 5 (2013), 1349-1356

Original Research

Phosphorus and Nitrogen Removal Using Novel Porous Bricks Incorporated with Wastes and Minerals

Dungang Gu, Xianzheng Zhu, Toulavanh Vongsay, Minsheng Huang*, Li Song, Yan He

Shanghai Key Laboratory of Urbanization and Ecological Restoration,
School of Resources and Environmental Sciences, East China Normal University, Shanghai, China

Received: 10 January 2013
Accepted: 28 May 2013

Abstract

In this study, wastes and minerals were incorporated into the production of bricks as a kind of water-purifying substrate. The brick contained 72% clay, 10% bagasse, 10% steel slag, 5% zeolite, and 3% calcite by weight. The brick exhibited highly and hierarchically porous structure. It can remove phosphate and ammonium simultaneously from aqueous solutions with the maximum adsorption amount of 3.8 mg/g for phosphate and 0.7 mg/g for ammonium. Kinetic analysis showed that the brick had a faster removal rate for phosphate than ammonium. The maximum desorbability of phosphate and ammonium were found to be 5.9% and 13.9%, respectively. Considering wastes recycling, easy fabrication, and favorable properties, this type of brick has the potential to be applied to in-situ remediation of aquatic environment.

Keywords: brick, waste recycling, phosphate, ammonium, removal

Introduction

The accumulation of nitrogen and phosphorus compounds in natural or artificial water bodies such as lakes, rivers, reserviors, and ponds is considered to be a major cause of eutrophication. Ammonium is recognized as one of the most common N-forms in wastewater [1], and phosphorus generally exists in orthophosphates [2]. When present in substantial quantities, these nutrients can cause excessive growth of algae, as well as a sharp decrease of dissolved oxygen and obvious fish toxicity [1-4]. Hence, it is of great importance for removing excess ammonium and phosphate from aquatic environments to control eutrophication.

Adsorption is an alternative method for treating nitrogen and phosphorus pollution due to its ready availability and low cost [1-7]. A lot of materials have been tested as adsorbents for ammonium and phosphate removal. Zeolite, a porous mineral described as crystalline hydrated aluminosilicates, can be effective in removing ammonium ions with the advantages of its three-dimensional framework structure, high ion exchange capacity, and good selectivity for ammonium [2-5]. Various iron, aluminum, or calcium-rich materials, such as steel slag [6], fly ash [7], opoka [8], wollastonite [9], and peat [10], have been widely investigated in removing phosphate.

However, there are still some disadvantages and limitations concerning these materials. Firstly, using only one material to adsorb phosphate and ammonium simultaneously from aqueous solutions is rarely reported. Ammonium ion (NH_4^+) is a cation whereas orthophosphate ion (PO_4^{3-}) is an anion, thus a combination of a cation exchanger and an anion exchanger (or an inorganic cohension precipitant) is needed to remove both NH_4^+ and PO_4^{3-} simultaneously [11]. Secondly, in a real engineering appli-

*e-mail: mshuang_ecnu@yahoo.com.cn

cation, adsorbents with fine particle sizes are comparatively hard to separate and replace. The random dumping of these materials as substrates in constructed wetlands will result in the problem of blocking. Besides, a certain mechanical strength is necessary for materials applied to lake and river revetments. Thirdly, some adsorbents may not be economically feasible in large-scale applications despite their good performance in adsorbing target pollutants because they are produced through complex synthesis or modification.

Brick is one of the oldest and most demanding building materials in the world [12]. Since energy saving and environmentally friendly waste recycling are both important issues, a variety of pore-forming agents have been incorporated into fired clay bricks to assist the production of porous and lightweight bricks over the past decades [13-18]. Most of these studies focus on the development of building material with optimized thermal conductivity and mechanical properties. Nevertheless, few studies have been reported regarding the application of brick as a water-purifying material in the restoration of aquatic environments.

This work investigated the feasibility of a novel porous brick for removing phosphorus and nitrogen from aquatic environments. Specifically, the brick was prepared with wastes (steel slag and bagasse) and natural minerals (zeolite and calcite) adding to clay in the conventional manufacturing process of fired clay bricks. The additional minerals are abundant, cheap, and easily obtainable in China. As for steel slag and bagasse, they are by-products and residues from steel plants and sugar mills, respectively. Large quantities of these wastes are produced annually, most of which are not adequately managed. Their utilization can be regarded as a resource reuse alternative in order to improve the water purification properties of the brick as well as reduce their disposal quantity and other negative environmental effects.

Materials and Methods

Materials

Clay was obtained from a brick manufacturing plant in Wenzhou, Zhejiang Province, China. Steel slag was acquired from a steel plant in Shanghai. Bagasse was collected from a sugar refinery in Wenzhou. Zeolite and calcite were supplied by a mining company in Jinyun, Zhejiang Province. The clay was air-dried, crushed, and passed through an 18-mesh sieve. Steel slag, zeolite, and calcite were prepared after crushing, grinding, and passing through a 40-mesh sieve. Bagasse was dried in sunlight until all the moisture evaporated and cut to 2-5 mm segements. The main chemical compositions of these raw materials analyzed via X-ray fluorescence (XRF-1800, Shimadzu, Japan) are listed in Table 1.

Table 1. Major chemical ingredients of the raw materials and the brick.

Sample	Chemical ingredient (%)						
	Fe_2O_3	CaO	K_2O	SiO_2	Al_2O_3	MgO	Na_2O
Clay	7.25	1.16	3.47	72.12	19.38	2.40	1.06
Steel slag	10.30	20.21	0.86	51.56	10.26	2.84	0.66
Zeolite	1.14	2.50	2.90	83.42	16.52	0.54	2.16
Calcite	0.17	53.81	0.18	1.57	0.34	2.34	—
Bagasse	8.04	5.37	11.35	52.71	1.74	5.42	1.16
Brick	7.59	3.98	3.28	70.29	18.23	2.38	1.52

Brick Specimen Processing

According to preliminary tests, the mixture contained 72% clay, 10% steel slag, 5% zeolite, 3% calcite, and 10% bagasse (mass%). The mixture was homogenized, blended, and molded in a 115 mm (L) × 60 mm (W) × 53 mm (H) mold. The specimens were air-dried at room temperature for 24 h and then dried to constant weight at 105ºC in an oven. The dried specimens were fired in a laboratory furnace at the rate of 2ºC/min until 600ºC, and then at 4ºC/min up to 850ºC for 2 h. Finally, the specimens were cooled to room temperature in the furnace.

Characterization of the Brick

A series of tests were carried out to determine physical properties, microstructure, and mineralogical composition. Archimedes' method was used to determine the bulk density and apparent porosity [17, 18]. Compressive strength was measured in accordance with ASTM C 67-07 standard [19]. Surface and interior morphology of the brick was observed using scanning electron microscopy (JSM-5610LV, JEOL, Japan). Chemical composition of the brick was analyzed by X-ray fluorescence (XRF-1800, Shimadzu, Japan). Crystalline phase of the brick was identified by X-ray diffraction (X'Pert Pro MPD, Philips, Netherland) in a 2θ range of 2-80º at a scanning rate of 2º/min.

Adsorption and Desorption Experiments

Phosphate and ammonium solutions were prepared by dissolving accurately weighed KH_2PO_4 and NH_4Cl in distilled water. Brick specimens were weighed respectively before use.

Batch equilibrium studies were carried out by putting one brick specimen into a series of 2 L beakers, respectively. Then the beakers were added with 1.2 L solutions containing different initial concentrations of PO_4^{3-}-P (50-2,000 mg/L) and NH_4^+-N (50-2,000 mg/L). The specimens were completely immersed in the solutions. Two drops of chloroform were added to each beaker to inhibit microbial activity, and pH was adjusted to 7. The beakers were sealed with Saran wrap, and then shaken on a horizontal shaker operating at 60 rpm and 25ºC for 7 d. At the end of this period, brick specimens were taken out and aqueous solutions were filtered through a 0.45 μm filter membrane.

The molybdenum blue method and Nesslerization method were employed to determine the concentrations of PO_4^{3-}-P and NH_4^+-N in the solutions, respectively [20].

In kinetics studies, the beaker contained a specimen into which 1.2 L solution was poured. The initial concentrations of PO_4^{3-}-P and NH_4^+-N were both 100 mg/L. The beakers were sealed and shaken at 25ºC immediately after adding two drops chloroform and adjusting pH to 7. Samples were taken for analyzing residual PO_4^{3-}-P and NH_4^+-N concentrations at different time intervals after the start.

The brick specimen previously used in the adsorption test with the maximum concentrations of PO_4^{3-}-P and NH_4^+-N was used for desorption studies. Experimental procedure was similar to that of kinetics studies except for using 1.2 L deionized water to substitute aqueous solution, and sampling at different times to measure the desorptive PO_4^{3-}-P and NH_4^+-N concentrations.

Removal efficiency, adsorption capacity (X), desorption capacity (Y) and desorption efficiency were calculated as per the following equations:

$$\text{Removal efficiency (\%)} = \frac{(C_0 - C_t)}{C_0} \times 100 \quad (1)$$

$$X = \frac{(C_0 - C_t)V}{m} \quad (2)$$

$$Y = \frac{C_t V}{m} \quad (3)$$

$$\text{Desorption efficiency (\%)} = \frac{Y}{X} \times 100 \quad (4)$$

...where C_0 and C_t are the initial and final solution concentrations (mg/L), respectively; V is the volume of the solution (L); and m is the weight of adsorbent used (g). All the data were determined in duplicate and reported as average values.

Results and Discussion

Characterization of the Brick

No particular problem was observed in the mixing, extrusion and drying steps of brick specimen processing. No cracking or bloating was observed after firing. There was no black core observed at the broken cross-section of the brick samples.

SEM images of the specimen at various magnifications are shown in Fig. 1. It is clearly seen from Fig. 1a that the surface of the brick is highly porous. Holes and pores of 0.2-200 μm in size can be seen clearly in the interior of the brick (Figs. 1b-d).

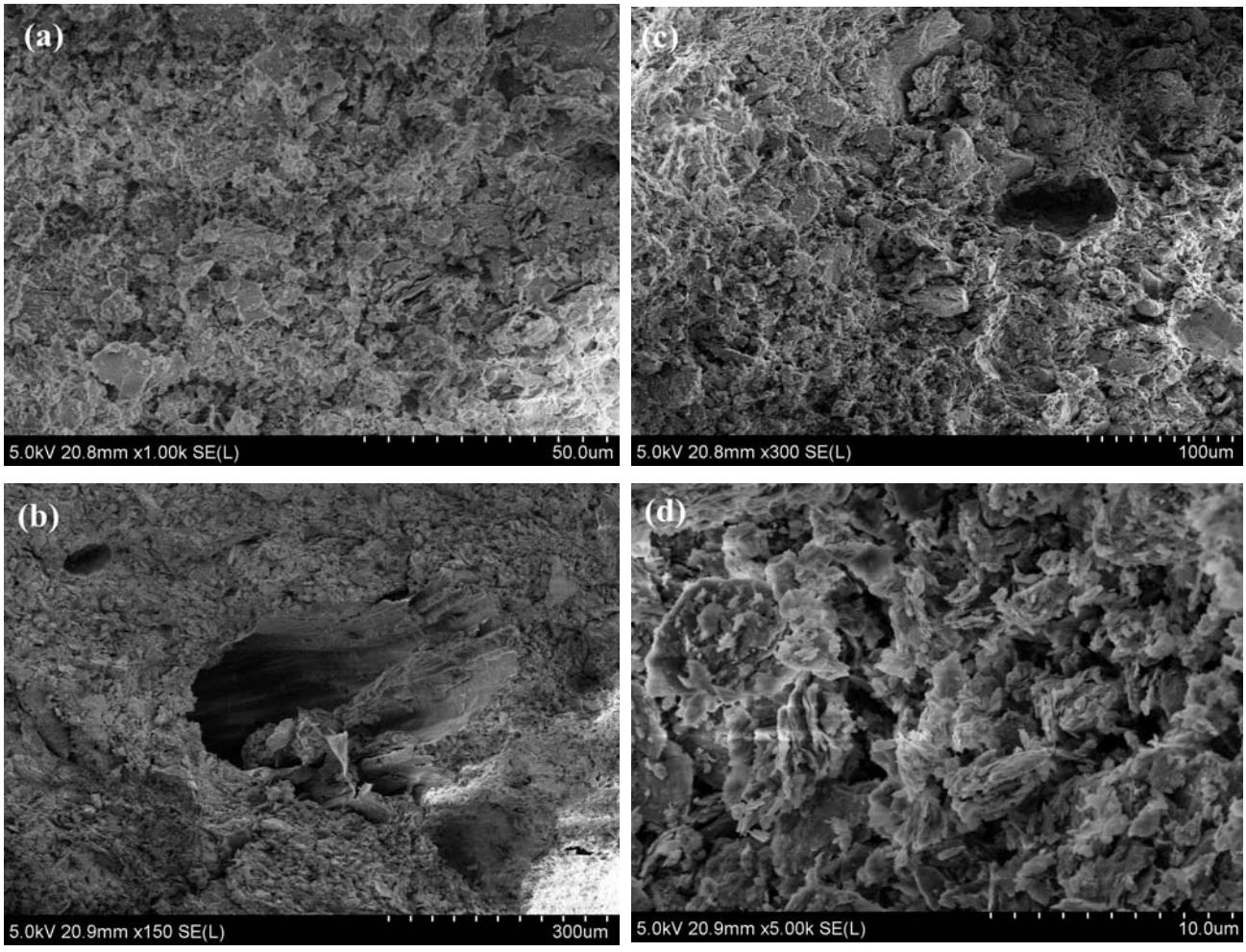

Fig. 1. SEM images of the porous brick surface (a) and interior (b-d).

Table 2. Pore size distribution of the brick.

Pore size range (μm)	Percentage (%)
< 0.2	2.82
0.2-0.5	14.11
0.5-0.8	12.10
0.8-1.0	11.29
1.0-2.0	19.35
2.0-3.0	9.27
3.0-4.0	4.84
4.0-5.0	7.66
5.0-10.0	12.50
10.0-50.0	4.44
> 50.0	1.61

Further analysis of SEM photographs using software Image J reveals the pore size distribution of the brick (Table 2). As a whole, the pores of the brick included large pores created by organic residue burning out and fine pores possessed by raw materials. Compared with single-sized pore materials, the material with different pore sizes integrated in one body may have improved properties [21]. The hierarchically porous structure can be expected to increase mass transport through the large pore channels as a consequence of reducing resistance to diffusion. Meanwhile, the fine pores can maintain highly specific surface areas for increasing adsorption sites and microbe habitats, which is in favor of extending the longevity of the brick for removing phosphate and ammonium.

The brick contained significant levels of SiO_2 (70.29%) and Al_2O_3 (18.23%), while the contents of other metal oxides were less than 10%. Fig. 2 shows that quartz was the main crystalline phase in the brick, which is in accord with the results of XRF analysis. The characteristic peaks of calcite were not observed from the XRD pattern, indicating that calcite had been decomposed after burning at sintering temperature.

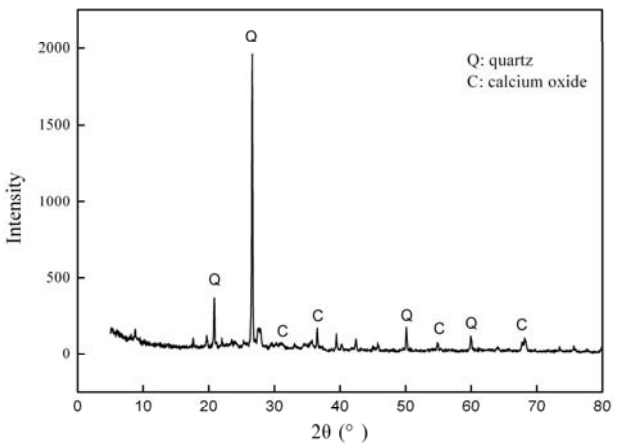

Fig. 2. XRD pattern of the porous brick.

The average bulk density of the bricks made for this study was 1.52 g/cm^3, slightly less than that of a common clay brick [13, 14]. Bulk density of bricks is related to the development of porosity during sintering. It is seen from the SEM images that the bricks exhibited fairly developed pore structure, which resulted in a comparatively light bulk density.

The average values of apparent porosity (% vol.) of the bricks were 46.94%. The incorporation of bagasse significantly increased porosity and produced large pores due to the buring out of organic matter. Demir [16, 17] and Sutcu [18] utilized various organic residues from industrial and agricultural waste as pore-forming agents to be incorporated in clay bricks. According to their findings, fired bricks with the addition of 10% paper processing residues, sawdust, tobacco residues, and grass exhibited apparent porosity of 38.9%, 42.2%, 41.3% and 41.8%, respectively. Compared with their research, the bricks manufactured in this study had a higher apparent porosity ratio. This can be attributed to gas emissions as the combustion of calcite and bagasse generated CO_2, which promoted the development of porosity. Furthermore, zeolite could also act as an inorganic pore-forming agent to increase the porosity of the brick. The fairly developed porosity not only increases specific surface area, but also provides more space for biofilm growth afterward to reinforce water purification.

In relation to mechanical properties, the average compressive strength of the fired samples was 8.3 MPa in our study. The compressive strength of the fired bricks depends on porosity content, shaping pressure, and sintering temperature, being decreased in the bricks containing organic residues or other pore-forming agents [16-18]. The National Standards of China (GB5101-2003) mandates a minimum compressive strength of 7.5 MPa for a common fired brick [22]. According to Yan [23], water-purifying media with compressive strength more than 1.5 MPa were feasible for transportation and utilization. Thus, the compressive strength of our brick is acceptable.

It is worth pointing out that energy consumption during firing could be lowered when recycling bagasse inside the brick due to its high calorific value of up to 2,200 kcal/kg (wet) [24], which provided heat to the combustion process.

Equilibrium Studies of Adsorptive Removal of Phosphate and Ammonium by the Brick

Fig. 3 and Fig. 4 show the equilibrium adsorption isotherms of phosphate and ammonium by the porous brick, respectively. The phosphate isotherm rises sharply with the phosphate equilibrium concentration increasing from 0 to 100 mg/L. With a further increase of the phosphate equilibrium concentration, the adsorption amount of phosphate was less significant. The ammonium adsorption capacity, however, seems to increase gently with the initial ammonium concentration increasing from 50 to 2000 mg/L. Two commly used empirical isotherm models, namely Freundlich and Langmuir [25] (as described in equations below) were tested in the present study for fitting the experimental data.

Table 3. Isotherm parameters for phosphate and ammonium adsorption by porous brick.

Adsorbate	Freundlich			Langmuir		
	K_f	n	R^2	q_m (mg/g)	b (L/g)	R^2
PO_4^{3-}-P	0.4087	3.0203	0.9657	3.7669	0.0138	0.9814
NH_4^+-N	0.0067	1.7445	0.9375	0.7284	0.0011	0.9730

$$q_e = K_f C_e^{1/n} \quad (5)$$

$$q_e = \frac{bq_m C_e}{1 + bC_e} \quad (6)$$

...where C_e (mg/L) is the equilibrium concentration and q_e (mg/g) is the amount of adsorbate sorbed at equilibrium. K_f and n are the Freundlich constants related to adsorption characteristics. q_m (mg/g) is the maximum adsorption capacity of a specific adsorbent, and b (L/g) is a Langmuir constant related to binding strength of adsorbate onto adsorbent. Isotherm parameters were determined through nonlinear regression and given in Table 3. The fitting curves of these two isotherms also are illustrated in Figs. 3 and 4.

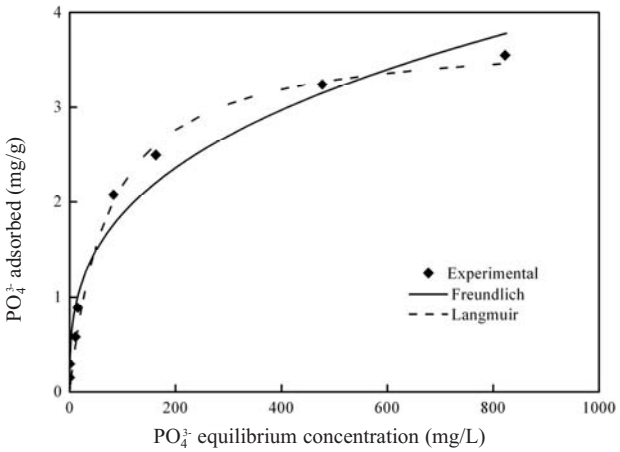

Fig. 3. Adsorption isotherm of phosphate by the porous brick.

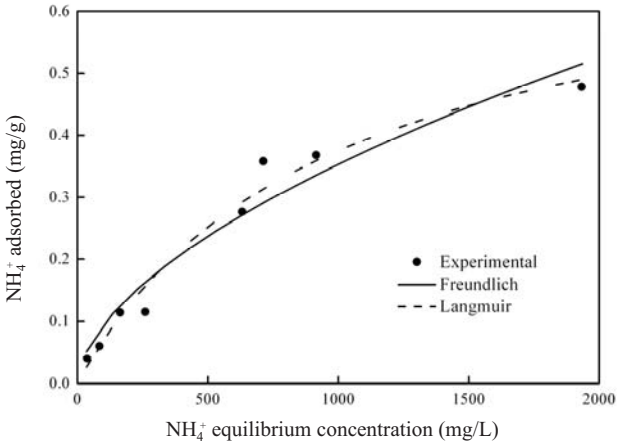

Fig. 4. Adsorption isotherm of ammonium by the porous brick.

Results showed that the experimental data of phosphate and ammonium adsorption onto the porous brick could be well fitted by both models. It can be seen in Figs. 3 and 4 that the Langmuir model fits the data better than the Freundlich model, which is consistent with the higher R^2 values of the Langmuir model than those of the Freundlich model.

In the Langmuir model, the constant b for phosphate adsorption was larger than that for ammonium adsorption, implying that our brick had a stronger affinity to phosphate than ammonium. The maximum amount of phosphate and ammonium adsorbed by the porous brick simultaneously at equilibrium was 3.8 mg/g and 0.7 mg/g, respectively. Similar results regarding phosphate and ammonium sorption capacity could be obtained from the Freundlich model by comparing K_f values. Besides, the constant n is related to the intensity of sorption. In this study, the values of n for both adsorbates were more than 1, suggesting that the adsorption conditions were favorable [4, 10].

Kinetics Studies of Adsorptive Removal of Phosphate and Ammonium by the Brick

It can be observed from Fig. 5 that the adsorption amount of phosphate increased significantly with the increase of contact time, consisting of fast and slow reaction processes. The fast reaction process was completed in 2 days, in which nearly 90% of the total phosphate in the aqueous solution was adsorbed. Then, as the slow reaction stage followed, the increase of adsorbed phosphate tended to diminish with adsorption amount reaching equilibrium. Our experiment showed that the porous brick could remove

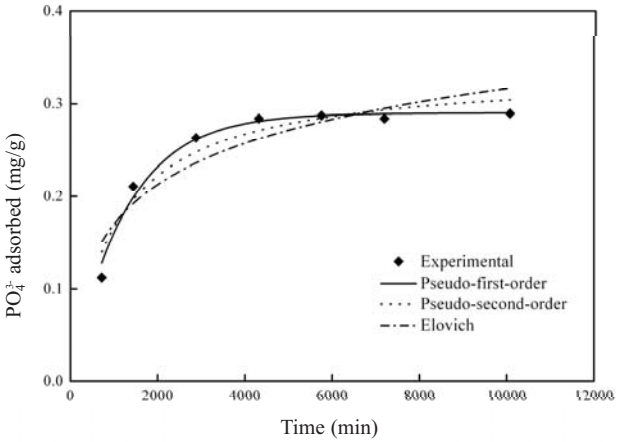

Fig. 5. Phosphate adsorption kinetics on the porous brick at initial phosphate concentration of 100 mg/L.

Table 4. Parameters and correlation coefficients (R^2) of various kinetic models.

Adsorbate	Pseudo-first-order			Pseudo-second-order			Elovich		
	q_1	k_1	R^2	q_2	k_2	R^2	α	β	R^2
PO_4^{3-}-P	0.2903	8.02×10^{-4}	0.9809	0.3347	2.95×10^{-3}	0.9241	8.07×10^{-4}	15.23	0.8186
NH_4^+-N	0.0497	1.19×10^{-4}	0.9733	0.0821	9.02×10^{-4}	0.9706	6.23×10^{-6}	29.88	0.9679

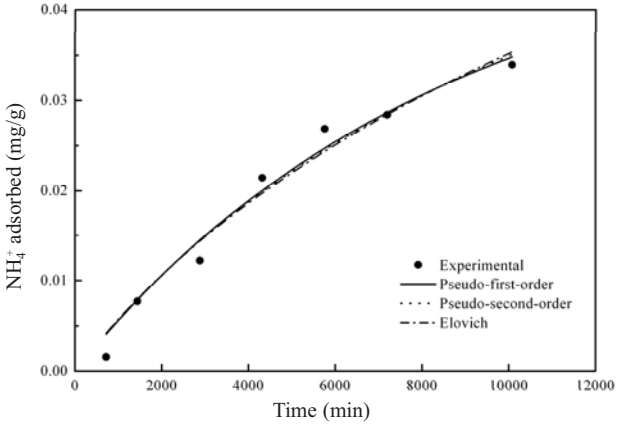

Fig. 6. Ammonium adsorption kinetics on the porous brick at initial ammonium concentration of 100 mg/L.

phosphate effectively and rapidly to reduce the potential ecological risk caused by high-level phosphorus. Fig. 6 suggests that the adsorption amount of ammonium increased slowly with the increase of contact time. The ammonium adsorption that was still increasing did not reach equlibrium after 7 days, thereby the removal of ammonium by our porous brick was an enduring process compared with the removal of phosphate.

In order to identify the types of adsorption mechanism, it is necessary to make a lumped analysis of kinetic data. In this study, Lagergren's pseudo-first-order model (Eq. (7)), Ho's pseudo-second-order model (Eq. (8)), and Elovich's model (Eq. (9)) were employed to predict the adsorption kinetics by means of non-linear fitting [26, 27]. The equations of these models are as follows:

$$q_t = q_1(1 - e^{-k_1 t}) \quad (7)$$

$$q_t = \frac{q_2^2 k_2 t}{1 + q_2 k_2 t} \quad (8)$$

$$q_t = \frac{1}{\beta}\ln(1 + \alpha\beta t) \quad (9)$$

...where q_t (mg/g) is the adsorption amount at time, q_1 (mg/g) and q_2 (mg/g) are the adsorption capacities at equilibrium, k_1 (1/min) and k_2 (g/mg min) are the pseudo-first and pseudo-second order rate constants, α (mg/g min) is the initial adsorption rate, and β (g/mg) is the desorption constant.

The fitting curves of the experimental kinetic results to the three models are shown in Figs. 5 and 6, and the estimated parameter values are presented in Table 4. In terms of phosphate sorption, the R^2 value for the pseudo-first-order kinetic model was the highest and the calculated q_1 value was in good agreement with the experimentally observed value. Therefore, the pseudo-first-order model is the best to represent the adsorption of phosphate by the porous brick. Regarding ammonium sorption, as shown in Fig. 6, all the three models seem to give a good fit to the experimental data. However, the pseudo-second-order model did not give an estimated q_2 value that was close to the experimental q_e value. Since the physical meaning should overwhlem the correlation coefficient [28], the pseudo-second-order model may not be very suitable to describe the kinetics of ammonium adsorbed onto the porous brick. The pseudo-first-order model is the most suitable for ammonium adsorption in light of the parameters and R^2 value.

Evaluation of Phosphate and Ammonium Desorption

The bricks used in desorption experiments were firstly adsorbed to saturation in equilibrium studies. Fig. 7 illustrates that both the desorbed phosphate and ammonium concentrations reached maximum in the third day and decreased in the fifth day. This decrease in desorbed sorbates can be explained by the resorption of them by the brick because adsorption-desorption processes are in dynamic balance. It is also seen that the concentrations of

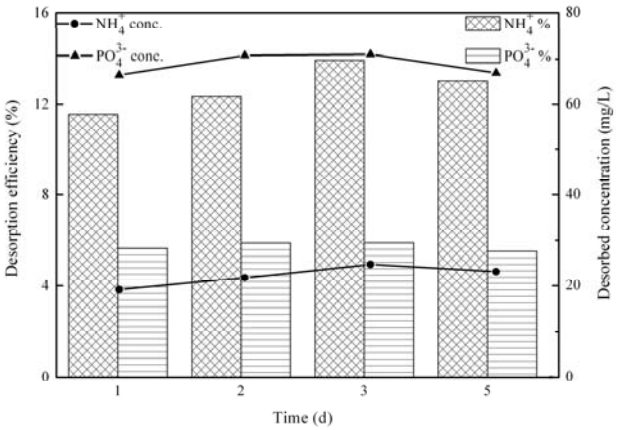

Fig. 7. Desorption efficiency of deionized water for the porous brick and desorbed concentration of phosphate and ammonium.

the desorbed phosphate and ammonium varied slightly during the desorption experiments, with more than 90% of the maximum desorption amount being achieved in 1 d, which implies that the desorption was a rapid process. The maximum phosphate and ammonium desorption efficiencies for the brick were 5.9% and 13.9%, respectively. As discussed earlier in equilibrium studies, the constant b in Langmuir model represents affinity between the sorbent and sorbate. Phosphate adsorption had a higher b value, implying that phosphate adsorbed on the brick was more difficult to be desorbed than ammonium. This prediction was confirmed by the observation that the porous brick had a higher desorption efficiency for ammonium than phosphate.

In addition, these results also indicate that the phosphate and ammonium adsorbed by the brick were not completely reversible. Since the bonding between the brick and adsorbed sorbates is relatively strong, the brick would not cause secondary pollution where large amounts of phosphate and ammonium are desorbed and released back to water.

As mentioned earlier, this study focused on the removal of nutrients by the porous brick itself without considering biological effects. In fact, if this material were applied in a real aquatic environment, biological activity would not be disregarded in pollutants removal, especially more important for the removal of nitrogen than phosphorus. The porous bricks can be microbial carriers due to their rough surface and numerous pores inside. With the increase of contact time, biofilm attaching on the surface and inner pores of the brick would reinforce the removal of nutrients. Additionally, microbes could utilize nutrients desorbed from the brick to maintain activity, which might promote the regeneration of the brick as an adsorbent. Hence, the porous brick can be a promising substrate for in-situ remediation of an aquatic environment.

Conclusion

The present study investigated the possibility of removing phosphate and ammonium simultaneously from aqueous solutions using a porous brick incorporated with wastes and minerals. The main conclusions can be drawn as follows:

1. The brick contained 72% clay, 10% bagasse, 10% steel slag, 5% zeolite, and 3% calcite by weight. Bagasse and calcite, serving as major pore-forming agents, decreased the bulk density and compressive strength while contributing to the formation of a highly and hierarchically porous structure with apparent porosity reaching 46.94%.
2. The maximum adsorption amount was 3.8 mg/g for phosphate and 0.7 mg/g for ammonium. The adsorption isotherms of both adsorbates were found to fit the Langmuir model better than the Freundlich model. The brick had a faster removal rate for phosphate than ammonium. The dynamic data for phosphate and ammonium adsorption can be predicted by the pseudo-first-order model.
3. The brick had a higher desorption efficiency for ammonium than phosphate. The low desorbability indicates that adsorbed phosphate and ammonium are relatively difficult to release back to water, which prevents the brick from becoming an endogenous pollution source.
4. The brick can serve as a microbial carrier in real application. Large-scale manufacture of this porous brick could be achieved easily based on a common fired brick plant. Incorporating agricultural residue and industrial waste into this brick also contributed to resource recycling and energy saving, providing economic and ecological benefits.

Acknowledgements

This work was supported by grants from the National Science and Technology Major Project of China on Water Pollution Treatment and Control (No. 2009ZX07317-006), the National Natural Science Foundation of China (Nos. 51278192, 41101471, 41001347), the Program of the Shanghai Subject Chief Scientist (No. 11XD1402100), and the Key Program of Shanghai Committee of Science and Technology (No. 12231201900).

References

1. EMARANON E., ULMANU M., FERNANDEZ Y., ANGER I., CASTRILLON L. Removal of ammonium from aqueous solutions with volcanic tuff. J. Hazard. Mater. **B137**, 1402, **2006**.
2. MONTALVO S.J., GUERRERO L.E., MILAN Z., BORJA R. Nitrogen and phosphorus removal using a novel integrated system of natural zeolite and lime. J. Environ. Sci. Heal. Pt. A. **46**, 1385, **2011**.
3. WEN D. H., HO Y.S., TANG X.Y. Comparative sorption kinetic studies of ammonium onto zeolite. J. Hazard. Mater. **B133**, 252, **2006**.
4. HUANG H.M., XIAO X.M., YAN B., YANG L.P. Ammonium removal from aqueous solutions by using natural Chinese (Chende) zeolite as adsorbent. J. Hazard. Mater. **175**, 247, **2010**.
5. WANG S.B., PENG Y.L. Natural zeolites as effective adsorbents in water and wastewater treatment. Chem. Eng. J. **156**, 11, **2010**.
6. DRIZO A., COMEAU Y., FORGET C., CHAPUIS R.P. Phosphorus saturation potential: A parameter for estimating the longevity of constructed wetlands systems. Environ. Sci. Technol. **36**, 4642, **2002**.
7. LU S.G., BAI S.Q., ZHU L., SHAN H.D. Removal mechanism of phosphate from aqueous solution by fly ash. J. Hazard. Mater. **161**, 95, **2009**.
8. BROGOWSKI Z., RENMAN G. Characterisation of opoka as a basis for its use in wastewater treatment. Pol. J. Environ. Stud. **13**, (1), 15, **2004**.
9. BROOKS A.S., ROZENWALD M.N., GEOHRING L.D., LION L. W., STEENHUIS T. S. Phosphorus removal by wollastonite: A constructed wetland substrate. Ecol. Eng. **15**, 121, **2000**.
10. XIONG J.B., MAHMOOD Q. Adsorptive removal of phosphate from aqueous media by peat. Desalination. **259**, 59, **2010**.

11. WU D.Y., ZHANG B.H., LI C.J., ZHANG Z.J., KONG H.N. Simultaneous removal of ammonium and phosphate by zeolite synthesized from fly ash as influenced by salt treatment. J. Colloid Interf. Sci. **304**, 300, **2006**.
12. CULTRONE G., SEBASTIAN E., CAZALLA O., NECHAR M., ROMERO R., BAGUR M.G. Ultrasound and mechanical tests combined with ANOVA to evaluate brick quality. Ceram. Int. **27**, 401, **2001**.
13. SHIH P.H., WU Z.Z., CHIANG H.L. Characteristics of bricks made from waste steel slag. Waste Manage. **24**, 1043, **2004**.
14. LIN K.L. Feasibility study of using brick made from municipal solid waste incinerator fly ash slag. J. Hazard. Mater. **B137**, 1810, **2006**.
15. HEREK L.C.S., HORI C.E., REIS M.H.M., MORA N.D., TAVARES C.R.G., BERGAMASCO R. Characterization of ceramic bricks incorporated with textile laundry sludge. Ceram. Int. **38**, 951, **2012**.
16. DEMIR I., BASPMAR M.S., ORHAN M. Utilization of kraft pulp production residues in clay brick production. Build. Environ. **40**, 1533, **2005**.
17. DEMIR I. Effect of organic residues addition on the technological properties of clay bricks. Waste Manage. **28**, 622, **2008**.
18. SUTCU M., AKKURT S. The use of recycled paper processing residues in making porous brick with reduced thermal conductivity. Ceram. Int. **35**, 2625, **2009**.
19. ASTM (American Society for Testing and Materials). Standard test methods for sampling and testing brick and structural clay tile (ASTM C 67-07), West Conshohocken, pp. 2-3, **2007**.
20. SEPAC (The State Environmental Protection Administration of China). Monitoring and Analytical Methods of Water and Wastewater. China Environmental Science Press: Beijing, pp. 243-281, **2002** [In Chinese].
21. SHAO G.S., LIU L., MA T.Y., YUAN Z.Y. Exotemplating synthesis of nitrogen-doped carbon materials with hierarchically porous structure and their application for lysozyme adsorption. Chem. Eng. J. **174**, 452, **2011**.
22. GAQSIQ (General administration of quality supervision, inspection and quarantine of P.R.China). National Standards of the People's Republic of China for Common Fired Bricks (GB 5101-2003), Beijing, pp. 2, **2003** [In Chinese].
23. YAN L. Research on the treatment of lakeside initial storm water runoff by the enhanced ecological engineering technology. Shanghai Jiao Tong University, pp. 74-75, **2006** [In Chinese].
24. USEPA (U.S.Environmental Protection Agency). Emission factor documentation for AP-42 section 1.8: Bagasse combustion in sugar mills, North Carolina, pp. 9, **1993**.
25. MEZENNER N.Y., BENSMAILI A. Kinetics and thermodynamic study of phosphate adsorption on iron hydroxide-eggshell waste. Chem. Eng. J. **147**, 87, **2009**.
26. MALASH G.F., EI-KHAIARY M.I. Methylene blue adsorption by the waste of Abu-Tartour phosphate rock. J. Colloid Interf. Sci. **348**, 537, **2010**.
27. DOTTO G.L., PINTO L.A.A. Adsorption of food dyes onto chitosan: Optimization process and kinetic. Carbohyd. Polym. **84**, 231, **2011**.
28. CHANG C.F., CHANG C.Y., CHEN K.H., TSAI W.T., SHIE J.L., CHEN Y.H. Adsorption of naphthalene on zeolite from aqueous solution. J. Colloid Interf. Sci. **277**, 29, **2004**.